



Cite this: DOI: 10.1039/d1cy00360g

The selective oxidation of glycerol over metal-free photocatalysts: insights into the solvent effect on catalytic efficiency and product distribution†

Pingbo Zhang, *^a Chengguang Yue,^a Mingming Fan,^{*a} Agus Haryonob,^b Yan Leng^a and Pingping Jiang ^a

Selective oxidation of glycerol to high value-added derivatives is a promising biomass conversion pathway, but the related reaction mechanism, in particular the solvent effect, is rarely studied. In this work, O-doped g-C₃N₄ was used as a metal-free catalyst to catalyze the selective oxidation of glycerol in different solvents. It was found that solvents can affect both catalytic efficiency and product distribution. A series of controlled experiments and theoretical calculation were applied to attest that the difference in interaction between glycerol and catalysts in different solvents is the main factor: competitive adsorption and hydrogen bond network from water inhibit the adsorption and activation of glycerol on the catalyst surface and reduce the conversion efficiency, while in acetonitrile, the stronger adsorption makes the oxidation reaction continue to yield esters. Two reaction routes in different solvents over O-doped g-C₃N₄ are proposed for the first time, which is helpful for people to better understand the related reaction mechanism.

Received 28th February 2021,
Accepted 19th March 2021

DOI: 10.1039/d1cy00360g

rsc.li/catalysis

Introduction

Due to the global energy crisis and environmental pollution, the development of green renewable energy is very rapid. As a green and renewable alternative to fossil fuels, biodiesel has become a popular biomass energy source, and its output has increased year by year. For every 10 tons of biodiesel produced, 1 ton of glycerol is produced as a by-product; as a result, the rapid development of the biodiesel industry has made the already saturated glycerin market even more sluggish.¹ The price of glycerol is continuously falling, making glycerol purification unprofitable; many factories choose to treat crude glycerin directly as waste, which not only leads to the waste of biomass resource, but also may cause environmental pollution. Therefore, the development of high value-added conversion methods for glycerol has become one of the current research hotspots in the field of biomass conversion.²

Among the reported high value-added conversion paths of glycerol, selective oxidation of glycerol is considered to be a

promising high value-added conversion method. Glycerol can be selectively oxidized to a variety of fine chemicals with high added values such as glyceraldehyde, glyceric acid, dihydroxyacetone, and hydroxypyruvate.³ Most studies on the aerobic oxidation of glycerol are focused on the traditional heterogeneous catalysis with noble metals as the active center of catalysts such as the Pt-Bi/C and Au/metal oxidation.^{4–8} Considering that noble metal catalysts have problems such as easy leaching and deactivation, and noble metals are scarce and expensive, the development of non-precious metal or metal-free catalysts with high activity shows better development prospects. In recent years, researchers have found that while using semiconductor materials with suitable valence band positions (such as Bi₂WO₆, Bi/Bi_{3.64}Mo_{0.36}O_{6.55}, and BiVO₄),^{9–11} glycerol can achieve photocatalytic aerobic oxidation on non-precious metal catalysts. However, there seems to be no report about the photocatalytic selective oxidation of glycerol using metal-free catalysts.

Metal-free catalysts such as carbon quantum dots, carbon nanotubes, graphenes, and graphitic carbon nitride are considered to be an important part of sustainable chemistry, considering they are rich in resources and stable in structure, and the unique physical and chemical properties of metal-free catalysts make them comparable to metal-containing catalysts in the catalytic fields of organic oxidation, hydrogen evolution, oxygen reduction, *etc.*^{12–15} It was reported that N-doped carbon nanotubes were applied as metal-free catalysts to catalyze the selective oxidation of glycerol using

^a The Key Laboratory of Synthetic and Biological Colloids, Ministry of Education, School of Chemical and Material Engineering, Jiangnan University, Wuxi 214122, P. R. China. E-mail: pingbozhang@126.com, fanmm2000@126.com

^b Research Center for Chemistry, Indonesian Institute of Sciences (LIPI), Kawasan Puspiptek, Serpong 15314, Indonesia

† Electronic supplementary information (ESI) available: Standard curves, LC-MS/MS methods, optimum geometries and catalyst characterization methods and results. See DOI: 10.1039/d1cy00360g

tert-butyl hydroperoxide as an oxidant, which can realize the highly selective conversion of glycerol into dihydroxyacetone.¹⁶ Inspired by the above-mentioned work, we supposed that a metal-free photocatalyst with a suitable valence conduction band position for activating oxygen and glycerol can be used to replace the nitrogen-containing carbon nanotubes to generate reactive oxygen species from oxygen under illumination, which may avoid the use of environment-unfriendly *tert*-butyl hydrogen peroxide to realize the selective oxidation of glycerol using a metal-free catalyst and oxygen. This catalytic reaction system should be more in line with the development concept of green and sustainable chemistry.

Polymeric graphitic carbon nitride (g-C₃N₄) as a metal-free semiconductor material, can achieve visible light response and participate in a variety of photocatalytic reactions owing to its suitable conduction and valence band edge positions, such as water splitting, carbon dioxide reduction, alcohol oxidation and degradation of organic pollutants.^{17–20} However, bulk g-C₃N₄ shows low photocatalytic efficiency due to its small specific surface area and high recombination rate of photo-induced electron-hole pairs.²¹ O-Doping is an efficient approach to improve the photocatalytic efficiency of g-C₃N₄; O-doped g-C₃N₄ has been widely applied in photocatalytic hydrogen production, pollutant degradation, organic matter transformation, hydrogen peroxide detection and other fields and has shown good catalytic performance.^{22–25} The reported oxygen-doping methods include acid treatment, hydrothermal, hydrogen peroxide oxidation and *in situ* calcination.^{26–29} Among them, the preparation process of *in situ* calcination is simple and easy, which does not need the participation of strong acids or concentrated hydrogen peroxide. By mixing a certain proportion of oxygen-doping sources such as ammonium acetate or other oxygen-rich organic substances in the precursor, oxygen atoms can be doped in the CN framework during the high-temperature calcination.

In the heterogeneous catalytic conversion of biomass, there are many factors that affect the results of the reaction, among which the solvent effect has been proven to play an important role on reaction rates and product selectivity.³⁰ Existing studies have shown that in the conversion of glucose into 5-hydroxymethylfurfural, as for increasing the amount of catalyst and increasing the reaction temperature to increase the conversion rate of the substrate, changing the reaction solvent can often achieve a multiplier effect with half the effort.^{31,32} In addition, the solvent effect can influence the distribution of products by modifying a solvent to selectively stabilize or destabilize a given product. Deng *et al.* discovered that the addition of water to the oxidative system can change the products of selective oxidative esterification of 5-(hydroxymethyl)furfural from dimethyl furan-2,5-dicarboxylate to methyl 5-(hydroxymethyl)furan-2-carboxylate.³³ In other polyol catalytic oxidation systems that own a similar structure to glycerol, researchers have found that water as a solvent affects the catalytic efficiency.

Carmine D'Agostino *et al.* found the competitive adsorption between the solvent water and the substrates in the catalytic oxidation of 1,3-propanediol and 1,4-butanediol, using nuclear magnetic resonance (NMR) relaxation time measurements.^{34,35} As a result, the conversion rate of the alcohols decreased significantly in the presence of water. It has been noticed that among the research results on the selective oxidation of glycerol in aqueous solutions that have been reported so far, the conversion rate of glycerol seems to be relatively low; hence, we speculate that water which as solvent in the glycerol selective oxidation system may have a certain impact on the catalytic efficiency. Moreover, considering that glycerol contains multiple hydroxyl groups, it is theoretically feasible for other derivative reactions (such as oxidative esterification) to occur in addition to oxidation under anhydrous conditions. However, there is little systematic study of elucidation of the solvent effect on the glycerol oxidation system, which is of great significance for the in-depth understanding of the reaction mechanism and the design and optimization of subsequent catalysts.

Herein, O-doped g-C₃N₄ (OCNN) prepared by an *in situ* calcination method was used as a metal-free catalyst to catalyze the selective oxidation of glycerol for the first time. The influence of solvent effect on the substrate conversion efficiency and product distribution was systematically investigated using different solvents and reference reactants. Moreover, to better understand the difference in the glycerol adsorption state on the OCNN surface under different solvent conditions from the molecular level, we conducted density functional theory (DFT) calculations using the Gaussian 16 software and independent gradient model (IGM) isosurface analysis with Multiwfn 3.6. A new reaction path: one-step oxidative esterification of glycerol to yield ester compounds was discovered and elucidated combining the characterizations by EPR and LC-MS/MS, which is helpful for people to better understand the reaction path and mechanism of photocatalytic oxidation of glycerol.

Experimental

Preparation of OCNNs

OCNNs were prepared according to the procedure reported in the literature²⁹ with some modifications. First, 10 g urea was mixed with different weights of ammonium acetate to get the precursors; the mixture was ground for 15 min and transferred into a 30 mL porcelain crucible with a cover and sealed with a tinfoil. Then, the sealed crucibles were calcined at 550 °C for 3 h at a heating rate of 10 °C min⁻¹ in a muffle furnace. The yellow solid in the crucible was taken out and ground into powder when the muffle furnace was naturally cooled to room temperature. These yellow powders were named OCN-1, OCN-2, OCN-3 and OCN-4, whose precursors contained different amounts of ammonium acetate (0.2, 0.4, 0.6 and 0.8 g, respectively). Finally, the OCNNs were moved into the porcelain crucible without any cover or tinfoil, and heated to 500 °C for 2 h at a ramping rate of 2 °C min⁻¹ in

the muffle furnace. The obtained nanosheets were named OCNN-1, OCNN-2, OCNN-3 and OCNN-4, whose precursors contained different amounts of ammonium acetate (0.2, 0.4, 0.6 and 0.8 g, respectively). In addition, the bulk $g\text{-C}_3\text{N}_4$ (CN) and $g\text{-C}_3\text{N}_4$ nanosheets (CNNs) were prepared by the same method as OCNs or OCNNs without the addition of ammonium acetate.

Photocatalytic oxidation of glycerol and propanediol

Typically, 10 mg catalyst was suspended in 5 mL of glycerol (or propanediol) acetonitrile solution (50 mmol L^{-1}) in a 25 mL round-bottomed flask. After the solution was bubbled with O_2 for 30 min, the flask was sealed with a balloon that was prefilled with O_2 and placed on the magnetic agitator with cold trap to maintain the temperature around $25 \text{ }^\circ\text{C}$. The reaction solution was illuminated using a 350 W Xe lamp (light intensity, 150 mW cm^{-2}) for a certain period. After the illumination, the mixture was centrifuged at 9500 rpm for 5 min to remove the catalyst particles; the suspension was collected and filtered through a $0.45 \text{ }\mu\text{m}$ nylon syringe filter. Then, the solution was analyzed using a high-performance liquid chromatograph (HPLC, Agilent 1100LC) equipped with a RID, and a Zorbax SAX column ($4.6 \text{ mm} \times 250 \text{ mm}$, Agilent) was used with a mixed solution of H_3PO_4 (0.5% v/v) in water/acetonitrile (1/2, v/v), (0.4 mL min^{-1}) as the eluent at $35 \text{ }^\circ\text{C}$, which was performed according to the procedure reported in the literature with some modifications.⁶ The amounts of consumed reactants and produced products were quantified by an external calibration method. The conversion of glycerol (or propanediol) and the selectivity of the main products were calculated using the following equations:

$$\text{Conversion} = [(C_0 - C)/C_0] \times 100\% \quad (1)$$

$$\text{Selectivity}_{(\text{main product})} = [C_m/(C_0 - C)] \times 100\% \quad (2)$$

where C_0 is the initial concentration of glycerol (or propanediol), and C and C_m are the concentrations of glycerol (or propanediol) and the main products, respectively, at a certain time after the photocatalytic reaction; the related standard curves of the detected substances were determined and shown in Fig. S1.† Besides, the chemical structures of some unknown products were confirmed by LC-MS/MS (AB SCIEX, X500R), and the details are shown in section 2 in the ESI.†

Simulation models and methods

For better studying the difference in the adsorption of glycerol on the OCNN surface under different solvent conditions, density functional theory (DFT) calculations were performed at the level of M062X/6-311 + G(d)^{36–38} using the Gaussian 16 software.³⁹ A dispersion correction for density functional theory (DFT-D3)⁴⁰ was adopted in the calculations for accurately describing the interactions. Before the DFT calculation, the structures of $g\text{-C}_3\text{N}_4$ ($Cmc2_1$ space group) and

substrates (glycerol, H_2O and CH_3CN) were fully optimized, and optimum geometries are shown in Fig. S4.† The SMD implicit solvent model⁴¹ was used to investigate the influence of the solvent in this system. One adsorbate molecule was introduced to the adsorption site of $g\text{-C}_3\text{N}_4$ to determine the adsorption configuration. The adsorption energy (E_a) of the adsorbed molecule was calculated using the following formula:

$$E_a = E_{\text{com}} - (E_{\text{ad}} + E_{\text{sub}}) \quad (3)$$

where E_{com} , E_{ad} and E_{sub} stand for the total energies of the complexes, adsorbent and substrate, respectively. In order to more intuitively analyze the adsorption of glycerol on $g\text{-C}_3\text{N}_4$ in different solvents, the interaction region and strength between substrate molecules and $g\text{-C}_3\text{N}_4$ were calculated using an independent gradient model (IGM) isosurface analysis⁴² with Multiwfn 3.6.⁴³ The IGM interaction regions and color-mapped isosurface graphs were obtained using the VMD 1.9.3 program.⁴⁴

Radical species trapping experiments

The mechanism of photocatalysis was investigated by a radical species trapping experiment to determine the main active species, which involved the photocatalytic oxidation process of glycerol. Different radical scavengers such as isopropanol, benzoquinone and furfuryl alcohol, which act as the scavenger of $\cdot\text{OH}$, O_2^- and $^1\text{O}_2$ respectively, were added to the photocatalytic oxidation system to detect the influence of the active species in the conversion process of glycerol under identical conditions. The change in glycerol conversion was taken as the important degree to evaluate the active species.

H_2O_2 determination

We referred to the literature and used potassium titanium(IV) oxalate as a detection agent to quantitatively analyze the

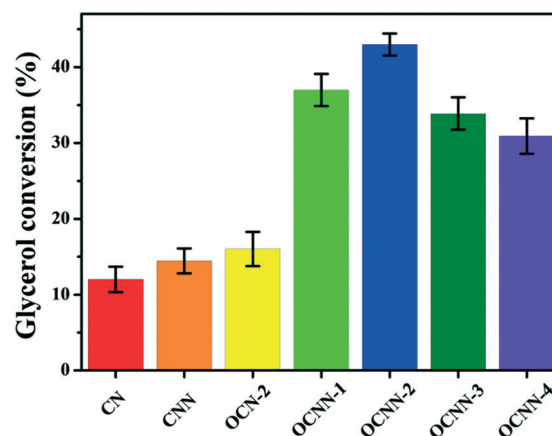


Fig. 1 Conversion of glycerol over different catalysts (reaction conditions: 5 mL 50 mM glycerol acetonitrile solution, 10 mg catalyst, O_2 , $20 \text{ }^\circ\text{C}$, 350 W Xe lamp, 1 h).

H₂O₂ content in the system.^{45,46} Briefly, 2 mL of the solution after 3 hours of reaction was taken out, the catalyst powder was removed using a 0.45 μm nylon syringe filter, 2 mL of potassium titanium oxalate solution (50 mmol L⁻¹) was added, and then 1 mL of ultrapure water was added to dilute the solution to 5 mL. The absorbance of the solution was obtained using an ultraviolet-visible spectrophotometer (Jinghua Instruments 752) at 400 nm. The H₂O₂ concentration was quantified by an external calibration method, and the standard curve of absorbance and hydrogen peroxide concentration is shown in Fig. S5.†

Results and discussion

First, we evaluated the activity of the prepared catalysts in a glycerol acetonitrile solution, and the results are shown in Fig. 1. It is clear that O-doping significantly improved the catalytic performance of g-C₃N₄ in this reaction system and the OCNN-2 catalyst showed the best catalytic performance (43.2% glycerol conversion in 1 h). A series of characterizations were performed to find out the effect of O-doping on the structure and properties of OCNN, as shown in section 4 in the ESI.† The results indicated that OCNN-2 has a thinner sheet structure, larger specific surface area, higher light absorption ability and lower photocarrier recombination rate, which is consistent with the results of the reported work,²⁵ and these changes are helpful to improve the catalytic performance.

The reactivity of glycerol on OCNN-2 in different solvents (acetonitrile, *N,N*-dimethylformamide, methanol and water) was explored, and the results are shown in Fig. 2a. It can be seen that as the polarity of the reaction solvent increases, the conversion rate of glycerol decreases significantly (43.2% in acetonitrile to 4.4% in water). Considering that the

adsorption strength of the substrate molecule on the surface of catalyst is related to the polarity, we believe that the strong polar solvent formed competitive adsorption with glycerol molecule on the surface of OCNN and blocked the reaction sites.

In order to verify the above-mentioned inference, we added a small amount of water into the glycerol acetonitrile solution to observe the effect of addition of different volumes of water on the glycerol conversion. The results are shown in Fig. 2b; as the volume of water increased (50, 200 and 500 μL), the conversion rate of glycerol was significantly reduced. In addition, we conducted the catalyst adsorption test to compare the adsorption of glycerol in acetonitrile and water over the same quality of the OCNN-2 catalyst (Fig. 2c). The results indicated that OCNN-2 adsorbed more glycerol molecules in the glycerol acetonitrile solution (3.9% in acetonitrile to 0.5% in water). The above-mentioned experimental results verify our speculation that strong polar solvents, such as water, can compete with glycerol molecules for adsorption on OCNN-2. The competitive adsorption will affect the adsorption and activation of glycerol molecules, which, in turn, reduces the catalytic efficiency of the reaction system. In addition, we compared the adsorption of glycerol on the CN and OCN-2 catalysts with similar specific surface areas (as shown in Fig. S6†). The results indicate that O-doping can increase the adsorption of glycerol on the surface of the catalyst. This may be due to the fact that O has a greater electronegativity than N, which facilitates the adsorption of glycerol molecules.

Considering that glycerol, as a polyol, has a complicated hydrogen bond network in its aqueous solution, it is generally believed that the existence of the hydrogen bond network will also affect the adsorption and activation of the substrate. Therefore, we speculated that in a glycerol aqueous solution, the existence of the hydrogen bond network is also a factor leading to the lower catalytic efficiency of the reaction system. To verify this conjecture, we used 1,2-propanediol (1,2-PG) and 1,3-propanediol (1,3-PG) as reference substrates, which possess fewer hydroxyl groups and thus the strength of hydrogen bond network in their aqueous solution is believed to be weaker than that of glycerol. The difference in reactivity between glycerol and propylene glycol in different solvents (acetonitrile and water) was investigated, and the results are shown in Fig. 2d. The results indicated that among the three aqueous alcohol solutions, the conversion rate of glycerol was the lowest and the conversion rate of 1,3-PG was the highest, which just showed a negative correlation with the strength of the

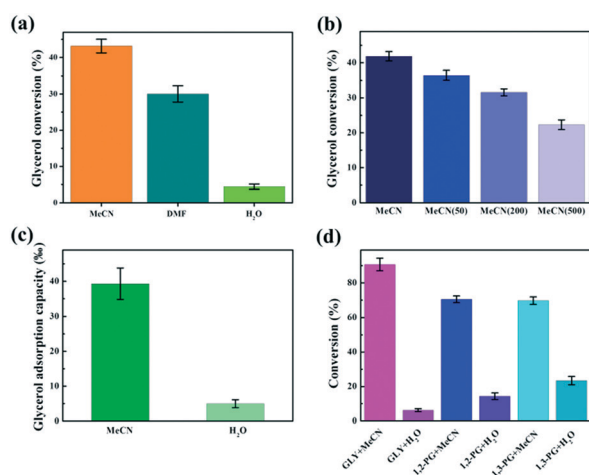
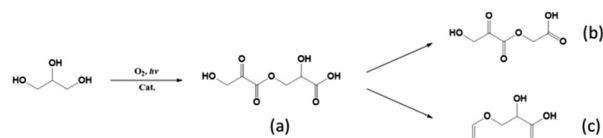


Fig. 2 (a) Glycerol conversion in different solvents. (b) Influence of adding different volumes of water on the reaction activity. (c) Adsorption of glycerol over OCNN in different solvents. (d) Alcohol conversion in acetonitrile or water (reaction conditions: 5 mL 50 mM alcohol solution, 10 mg OCNN-2, O₂, 20 °C, 350 W Xe lamp, 1 h for (a) and (b) and 3 h for (d)).



Scheme 1 Presumed reaction path of the esters in the reaction system.

Table 1 Results of photocatalytic oxidation of glycerol and propylene glycol in the aqueous solution

Reactant	Conversion (%)	Products concentration (mM L ⁻¹) and selectivity (%)		
Glycerol	6.0	DHA 1.8 (62.6)	GLAD 0.5 (15.7)	Others 21.7
1,2-Propanediol	14.5	LA 5.6 (76.8)		Others 23.2
1,3-Propanediol	23.7	3-HPA 16.0 (85.5)		Others 14.5

Reaction conditions: 5 mL 50 mM alcohols aqueous solution, 10 mg cat., O₂, 20 °C, 350 W Xe lamp, 3 h.

hydrogen bond network in the aqueous solutions of the three alcohols. This negative correlation indicated that the hydrogen bond network did affect the reactivity of polyols in the system. Another interesting phenomenon was that the glycerol acetonitrile solution showed the highest conversion rate, while the conversion rate of the propylene glycols was basically the same. This phenomenon indicated that the reactivity of alcohols on the OCN surface was related to the polarity of its molecular structure (glycerol molecules have more hydroxyl groups than propylene glycol) without the existence of solvent competitive adsorption or hydrogen bond network in polyol acetonitrile solution, which proved that the adsorption activation of hydroxyls on the catalyst surface is a key step in the photocatalytic oxidation of glycerol and propylene glycol.

Except the solvent effect on the glycerol conversion rate, it was found that different solvents also affected the distribution of oxidation products in the polyol reaction system, particularly for glycerol. We detected several ester compounds in the reaction system of the glycerol acetonitrile solution and completed the preliminary characterization of the new compounds using LC-MS/MS for the first time. The measured molecular weight was basically consistent with the calculated molecular weight (Table S1†). Moreover, the compound structural formulas of these esters were confirmed using the MS/MS fragments of the parent ions (Fig. S2†), and we presumed that these esters can achieve progressive

transformation through the cleavage of carbon-carbon bonds, as shown in Scheme 1.

Table 1 shows the results of photocatalytic oxidation of glycerol and propylene glycol aqueous solution. The main products of glycerol were dihydroxyacetone (DHA, 62.6% in selectivity), glyceraldehyde (GLAD, 15.7% in selectivity), and hydroxypyruvaldehyde (HPAD, the presence of this substance was confirmed by LC-MS as shown in Fig. S3†). The oxidation products of propylene glycol were mainly hydroxypropionic acid compounds (lactic acid (LA, 76.8% in selectivity) for 1,2-PG and 3-hydroxypropionic acid (3-HPA, 85.5% in selectivity) for 1,3-PG). It should be noticed that the oxidation products of glycerol were aldehydes and ketones, and no acidic compound was found. We speculated that the existence of the strong hydrogen bond network in the glycerol aqueous solution promoted desorption of the products and prevented the further oxidation of glycerol-oxidized derivatives to acids in this reaction system.

Different from the high selectivity of C₃ products in the aqueous solution, the oxidation products of the alcohol acetonitrile solution showed more C₂ and C₁ products generated by the cleavage of the carbon-carbon bond. We recorded the substrate conversion rate and product distribution as the reaction time increased in the polyol acetonitrile solution, as shown in Fig. 3. The composition of the oxidation products in the glycerol acetonitrile solution was relatively complicated (Fig. 3a). In addition to the above-mentioned ester products, we discovered other glycerol oxidation derivatives such as formic acid (FA), glycolic acid (GLCA), dihydroxyacetone (DHA), glyceraldehyde (GLAD), glyceric acid (GLA) and hydroxypyruvaldehyde (HPAD). It can be seen that as the reaction time prolonged, the concentration of FA in the system gradually increased. The concentration of DHA and GLCA increased within 2 h and then decreased, indicating that DHA and GLCA were further oxidized to other products. Although the presence of GLA and GLAD were detected in the system, the content was very low and the concentration change was not obvious,

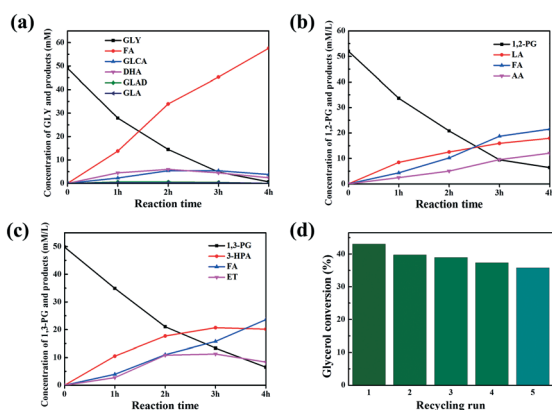


Fig. 3 Results of photocatalytic oxidation of glycerol (a), 1,2-PG (b), and 1,3-PG (c) in the acetonitrile solution and stability test of OCN-2 in the glycerol acetonitrile solution (d) (reaction conditions: 5 mL 50 mM alcohol acetonitrile solution, 10 mg cat., O₂, 20 °C, 350 W Xe lamp).

Table 2 Adsorption energy of the substrates on g-C₃N₄ in different solvents

Solvent	Substrate	Adsorption energy (kJ mol ⁻¹)
Water	H ₂ O	-24.6
	Glycerol	-49.8
Acetonitrile	CH ₃ CN	-7.7
	Glycerol	-45.2

indicating that GLA and GLAD were intermediate products in the glycerol oxidation process and will be quickly converted into other compounds. It is worth noting that hydroxypyruvate was not detected in the system, and hence, we speculated that the ester 2-hydroxy-3-((3-hydroxy-2-oxopropanoyl)oxy)propanoic acid was obtained from HPAD, which acted as the precursor. The main oxidation products of propylene glycols in the acetonitrile solution were hydroxypropionic acids (LA for 1,2-PG and 3-HPA for 1,3-PG) in the beginning. Then, C2 products (acetic acid (AA) and ethanol (ET)) and C1 products (formic acid) were formed owing to the peroxidation of the main products as the reaction preceded; the details are shown in Fig. 3b and c. Finally, we tested the stability of the OCNN-2 catalyst, as shown in Fig. 3d. The result indicated that OCNN-2 still maintained more than 80% catalytic activity after repeated use for five times.

In brief, in this glycerol photocatalytic reaction system, when water was used as a solvent, the adsorption and activation of glycerol substrate molecules on the catalyst surface was inhibited due to the existence of competitive adsorption and hydrogen bond network, which made the catalytic efficiency low, while the timely desorption of the oxidation product in the aqueous solution avoided the peroxidation of the oxidation product, which made the selectivity of C3 product (DHA) relatively high. As for the glycerol acetonitrile system, due to the efficient adsorption of substrate molecules on the surface of OCNN-2, the catalytic efficiency became higher, but the desorption of oxidation products in the weakly polar solvent acetonitrile solution was relatively slow, which resulted in the C3 oxidation products participating in the next esterification or peroxidation reaction to generate ester compounds or C2 and C1 products.

To better understand the difference in the glycerol adsorption state on the OCNN surface under different solvent conditions from the molecular level, we conducted density functional theory (DFT) calculations using the Gaussian 16 software³² to figure out the adsorption energy of the substrates on $g\text{-C}_3\text{N}_4$ in different solvents. The related results based on the interaction models (as shown in Fig. S4†) are given in Table 2. As we can see, the adsorption energy

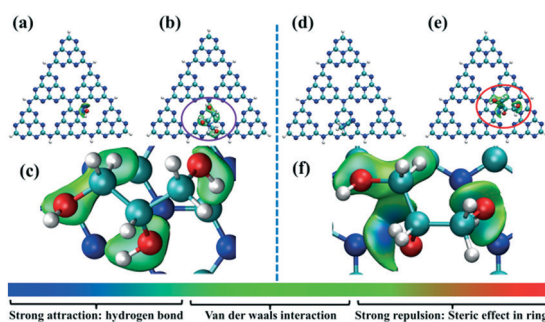


Fig. 4 IGM isosurface color maps of different adsorption configurations: (a) H_2O and (b) glycerol on $g\text{-C}_3\text{N}_4$ in water and (c) the enlargement of the circle in (b); (d) CH_3CN and (e) glycerol on $g\text{-C}_3\text{N}_4$ in acetonitrile and (f) the enlargement of the circle in (e).

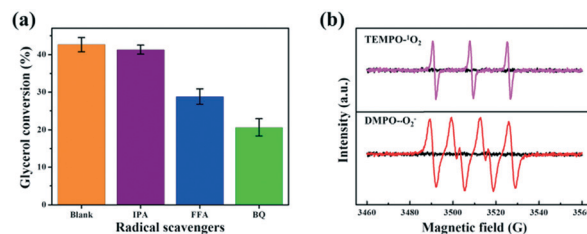


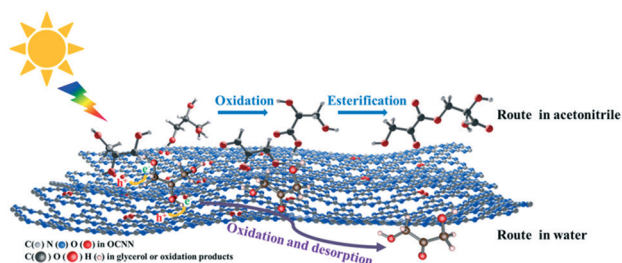
Fig. 5 (a) Results of controlled experiments using different active oxygen radical scavengers. (b) EPR spectra of the singlet oxygen and superoxide radicals over OCNN-2 (isopropanol (IPA) as a scavenger for hydroxyl radicals; furfural alcohol (FFA) as a scavenger for singlet oxygen; *p*-benzoquinone (BQ) as a scavenger for superoxide radicals).

between the CH_3CN molecule and $g\text{-C}_3\text{N}_4$ was significantly smaller than that of glycerol in the acetonitrile solvent, which indicated that CH_3CN molecules could not form competitive adsorption with glycerol molecules on the catalyst surface; while in water, due to the presence of the hydroxyl group with strong polarity in the structure of H_2O molecules, the interaction between H_2O and $g\text{-C}_3\text{N}_4$ is significantly greater than that of CH_3CN but less than that of glycerol, but it should be noticed that the volume of glycerol molecules is significantly larger than that of H_2O ; in other words, the adsorption energies of four or five H_2O molecules (approximately equal to the size of one glycerol molecule) must be stronger than that of one glycerol molecule. This result indicated that it is possible to form competitive adsorption between solvent water and glycerol molecule on the catalyst surface.

Additionally, the weak interactions between the substrates and $g\text{-C}_3\text{N}_4$ were calculated using the independent gradient model (IGM) approach,³⁵ and the results are shown in Fig. 4. As observed, when water was used as the solvent, the interactions between H_2O molecules and $g\text{-C}_3\text{N}_4$ (Fig. 4a) involved hydrogen bonding (shown in blue) and van der Waals forces (shown in green), while the interaction between the glycerol molecule and $g\text{-C}_3\text{N}_4$ (Fig. 4b) only involved van der Waals forces (shown in green). This result indicated that the interaction of H_2O and $g\text{-C}_3\text{N}_4$ is stronger than that of the glycerol molecule in water. When the solvent water was replaced with acetonitrile, the interaction between the $\text{CH}_3\text{-CN}$ molecule and $g\text{-C}_3\text{N}_4$ (Fig. 4d) was much weaker, which was consistent with the calculated result of adsorption energy. Without the interference of strong polar solvent water, the interaction between the glycerol molecule and $g\text{-C}_3\text{N}_4$ (Fig. 4e) showed a stronger interaction (hydrogen bonding interaction, shown in blue) besides van der Waals interaction (shown in green). The specific distinction of the

Table 3 Concentration of H_2O_2 during the photocatalytic reaction in acetonitrile

Substrate	Glycerol	1,2-PG	1,3-PG
Conversion (%)	90.7	70.4	69.6
$\text{C}_{\text{H}_2\text{O}_2}$ ($\mu\text{mol L}^{-1}$)	1117.1	671.1	671.1



Scheme 2 Possible photocatalytic reaction routes for glycerol oxidation over OCNN-2 in water and acetonitrile.

interactions between the glycerol molecule and $g\text{-C}_3\text{N}_4$ in water or acetonitrile can be clearly seen in Fig. 4c and f; this result indicated that glycerol showed a stronger interaction on the catalyst surface in the acetonitrile solvent, which was beneficial for the adsorption and activation of glycerol molecules and improve the conversion of glycerol.

In order to ascertain the active oxygen species playing major roles in the photocatalytic oxidation system of the glycerol–acetonitrile solution, we carried out active radical capture experiments and EPR characterization. In Fig. 5a, the addition of furfural alcohol (singlet oxygen scavenger) and *p*-benzoquinone (superoxide radical scavenger) resulted in a decrease in the conversion rate of glycerol, while the addition of isopropanol as a hydroxyl radical scavenger showed almost no change in the conversion rate of glycerol. At the same time, in the EPR spectra of the OCNN-2 catalyst (Fig. 5b), obvious signals of singlet oxygen and superoxide radicals were observed, indicating that these two active oxygen species were produced in the system. The above results showed that singlet oxygen and superoxide radicals participated in the photocatalytic oxidation process of glycerol and acted as main reactive oxygen species in this system.

To figure out the product of molecular oxygen in this catalytic system, we carried out the H_2O_2 determination in the solution after the reaction, and the results are given in Table 3. It can be seen that there is a certain amount of H_2O_2 in the polyol acetonitrile solution after the reaction, and the content of H_2O_2 is proportional to its conversion rate; hence, we speculate that oxygen will become H_2O_2 after participating in the reaction. With reference to the existing reports in the literature,^{47,48} we believe that H_2O_2 is produced *via* two-electron reduction of O_2 . In addition, the concentration of H_2O_2 in the system is relatively low, which may be due to the faster decomposition of H_2O_2 in an anhydrous environment.⁴⁷

Combining the above-mentioned results, the possible photocatalytic routes for glycerol oxidation over OCNN-2 are proposed, as shown in Scheme 2. Glycerol molecules adsorbed on the surface of the catalyst can be activated and oxidized to oxidation products under the interaction of photogenic holes and reactive oxygen species. In aqueous solutions, the oxidation products (mainly DHA and GLAD) quickly desorbed from the surface of the catalyst, thereby avoiding the occurrence of peroxides or other side reactions.

While in the acetonitrile solution, glycerol molecules strongly adsorbed on the catalyst surface, which were oxidized to form HPAD and GLAD, which could not desorb immediately and further the esterification reaction occurred to generate 2-hydroxy-3-((3-hydroxy-2-oxopropanoyl)oxy)propanoic acid or other compounds.

Conclusions

A green and sustainable conversion route for the selective oxidation of glycerol and its polyol derivatives at ambient temperature and atmosphere with molecular oxygen as the oxidant on a metal-free catalyst (O-doped $g\text{-C}_3\text{N}_4$) under illumination was provided in this work. Through a series of controlled experiments and theoretical calculation, we systematically studied the solvent effect on this catalytic reaction system at the molecular level. It was found that the interaction between glycerol and the catalyst surface was significantly different in different solvent environments, leading to different conversion efficiencies and product distributions. Through the active radical capture experiments and EPR characterization, we investigated the reaction mechanism of this system, and singlet oxygen and superoxide radical were proved as the main reactive oxygen species. The oxidation reaction path of glycerol in different solvents was given. In particular, it has been found for the first time that the oxidative esterification reaction can occur to generate new ester compounds in the glycerol acetonitrile solution. These findings should have certain reference values for the subsequent design and development of related catalysts.

Conflicts of interest

There are no conflicts to declare.

Acknowledgements

The financial supports from the Natural Science Foundation of China (NSFC) (No. 21978112) and MOE & SAFEA for the 111 Project (B13025) are gratefully acknowledged.

References

- 1 C. H. Zhou, J. N. Beltramini, Y. X. Fan and G. Q. Lu, *Chem. Soc. Rev.*, 2008, **37**, 527–549.
- 2 B. Katryniok, H. Kimura, E. Skrzyńska, J.-S. Girardon, P. Fongarland, M. Capron, R. Ducoulombier, N. Mimura, S. Paul and F. Dumeignil, *Green Chem.*, 2011, **13**, 1960–1979.
- 3 G. Dodekatos, S. Schünemann and H. Tüysüz, *ACS Catal.*, 2018, **8**, 6301–6333.
- 4 Y. Wang, D. Yuan, J. Luo, Y. Pu, F. Li, F. Xiao and N. Zhao, *J. Colloid Interface Sci.*, 2020, **560**, 130–137.
- 5 F.-F. Wang, S. Shao, C.-L. Liu, C.-L. Xu, R.-Z. Yang and W.-S. Dong, *Chem. Eng. J.*, 2015, **264**, 336–343.
- 6 D. Liang, J. Gao, H. Sun, P. Chen, Z. Hou and X. Zheng, *Appl. Catal., B*, 2011, **106**, 423–432.

- 7 H. Kimura, *Appl. Catal., A*, 1993, **105**, 147–158.
- 8 P. Yang, J. Pan, Y. Liu, X. Zhang, J. Feng, S. Hong and D. Li, *ACS Catal.*, 2018, **9**, 188–199.
- 9 D. Liu, J. C. Liu, W. Cai, J. Ma, H. B. Yang, H. Xiao, J. Li, Y. Xiong, Y. Huang and B. Liu, *Nat. Commun.*, 2019, **10**, 1779.
- 10 Y. Zhang, N. Zhang, Z.-R. Tang and Y.-J. Xu, *Chem. Sci.*, 2013, **4**, 1820–1824.
- 11 S. Zhao, Z. Dai, W. Guo, F. Chen, Y. Liu and R. Chen, *Appl. Catal., B*, 2019, **244**, 206–214.
- 12 D. S. Su, J. Zhang, B. Frank, A. Thomas, X. Wang, J. Paraknowitsch and R. Schloegl, *ChemSusChem*, 2010, **3**, 169–180.
- 13 J. Long, X. Xie, J. Xu, Q. Gu, L. Chen and X. Wang, *ACS Catal.*, 2012, **2**, 622–631.
- 14 L. Dai, Y. Xue, L. Qu, H.-J. Choi and J.-B. Baek, *Chem. Rev.*, 2015, **115**, 4823–4892.
- 15 M. Z. Rahman, M. G. Kibria and C. B. Mullins, *Chem. Soc. Rev.*, 2020, **49**, 1887–1931.
- 16 N. Gupta, O. Khavryuchenko, A. Villa and D. Su, *ChemSusChem*, 2017, **10**, 3030–3034.
- 17 X. Wang, S. Blechert and M. Antonietti, *ACS Catal.*, 2012, **2**, 1596–1606.
- 18 S. Cao, J. Low, J. Yu and M. Jaroniec, *Adv. Mater.*, 2015, **27**, 2150–2176.
- 19 Y. Zheng, L. Lin, B. Wang and X. Wang, *Angew. Chem., Int. Ed.*, 2015, **54**, 12868–12884.
- 20 Y. Xu, Z. Zhang, C. Qiu, S. Chen, X. Ling and C. Su, *ChemSusChem*, 2021, **14**, 582–589.
- 21 W. J. Ong, L. L. Tan, Y. H. Ng, S. T. Yong and S. P. Chai, *Chem. Rev.*, 2016, **116**, 7159–7329.
- 22 W. Zhu, N. Hao, J. Lu, Z. Dai, J. Qian, X. Yang and K. Wang, *Chem. Commun.*, 2020, **56**, 1409–1412.
- 23 Y. Huang, L. Ning, Z. Feng, G. Ma, S. Yang, Y. Su, Y. Hong, H. Wang, L. Peng and J. Li, *Environ. Sci.: Nano*, 2021, **8**, 460–469.
- 24 J. Ma, D. Jin, Y. Li, D. Xiao, G. Jiao, Q. Liu, Y. Guo, L. Xiao, X. Chen, X. Li, J. Zhou and R. Sun, *Appl. Catal., B*, 2021, **283**, 119520.
- 25 G. Q. Zhang, Y. S. Xu, C. X. He, P. X. Zhang and H. W. Mi, *Appl. Catal., B*, 2021, **283**, 119636.
- 26 H. Wang, S. Jiang, S. Chen, D. Li, X. Zhang, W. Shao, X. Sun, J. Xie, Z. Zhao, Q. Zhang, Y. Tian and Y. Xie, *Adv. Mater.*, 2016, **28**, 6940–6945.
- 27 Q. Gao, J. Xu, Z. Wang and Y. Zhu, *Appl. Catal., B*, 2020, **271**, 118933.
- 28 W. Jiang, Q. Ruan, J. Xie, X. Chen, Y. Zhu and J. Tang, *Appl. Catal., B*, 2018, **236**, 428–435.
- 29 F. Li, M. Han, Y. Jin, L. Zhang, T. Li, Y. Gao and C. Hu, *Appl. Catal., B*, 2019, **256**, 117705.
- 30 L. Shuai and J. Luterbacher, *ChemSusChem*, 2016, **9**, 133–155.
- 31 H. Zhao, J. E. Holladay, H. Brown and Z. C. Zhang, *Science*, 2007, **316**, 1597–1600.
- 32 Y. J. Pagán-Torres, T. Wang, J. M. R. Gallo, B. H. Shanks and J. A. Dumesic, *ACS Catal.*, 2012, **2**, 930–934.
- 33 K. S. Kozlov, L. V. Romashov and V. P. Ananikov, *Green Chem.*, 2019, **21**, 3464–3468.
- 34 C. D'Agostino, M. R. Feaviour, G. L. Brett, J. Mitchell, A. P. E. York, G. J. Hutchings, M. D. Mantle and L. F. Gladden, *Catal. Sci. Technol.*, 2016, **6**, 7896–7901.
- 35 C. D'Agostino, T. Kotionova, J. Mitchell, P. J. Miedziak, D. W. Knight, S. H. Taylor, G. J. Hutchings, L. F. Gladden and M. D. Mantle, *Chem. – Eur. J.*, 2013, **19**, 11725–11732.
- 36 R. Krishnan, J. S. Binkley, R. Seeger and J. A. Pople, *J. Chem. Phys.*, 1980, **72**, 650–654.
- 37 T. Clark, J. Chandrasekhar, G. W. Spitznagel and P. V. R. Schleyer, *J. Comput. Chem.*, 1983, **4**, 294–301.
- 38 Y. Zhao and D. G. Truhlar, *Theor. Chem. Acc.*, 2008, **120**, 215–241.
- 39 M. J. Frisch, G. W. Trucks, H. B. Schlegel, G. E. Scuseria, M. A. Robb, J. R. Cheeseman, G. Scalmani, V. Barone, G. A. Petersson, H. Nakatsuji, X. Li, M. Caricato, A. V. Marenich, J. Bloino, B. G. Janesko, R. Gomperts, B. Mennucci, H. P. Hratchian, J. V. Ortiz, A. F. Izmaylov, J. L. Sonnenberg, D. Williams-Young, F. Ding, F. Lipparini, F. Egidi, J. Goings, B. Peng, A. Petrone, T. Henderson, D. Ranasinghe, V. G. Zakrzewski, J. Gao, N. Rega, G. Zheng, W. Liang, M. Hada, M. Ehara, K. Toyota, R. Fukuda, J. Hasegawa, M. Ishida, T. Nakajima, Y. Honda, O. Kitao, H. Nakai, T. Vreven, K. Throssell, J. A. Montgomery, Jr., J. E. Peralta, F. Ogliaro, M. J. Bearpark, J. J. Heyd, E. N. Brothers, K. N. Kudin, V. N. Staroverov, T. A. Keith, R. Kobayashi, J. Normand, K. Raghavachari, A. P. Rendell, J. C. Burant, S. S. Iyengar, J. Tomasi, M. Cossi, J. M. Millam, M. Klene, C. Adamo, R. Cammi, J. W. Ochterski, R. L. Martin, K. Morokuma, O. Farkas, J. B. Foresman and D. J. Fox, *Gaussian 16, Revision C.01*, Gaussian, Inc., Wallingford CT, 2019.
- 40 S. Grimme, J. Antony, S. Ehrlich and H. Krieg, *J. Chem. Phys.*, 2010, **132**, 154104.
- 41 A. V. Marenich, C. J. Cramer and D. G. Truhlar, *J. Phys. Chem. B*, 2009, **113**, 6378–6396.
- 42 C. Lefebvre, G. Rubez, H. Khartabil, J. C. Boisson, J. Contreras-Garcia and E. Henon, *Phys. Chem. Chem. Phys.*, 2017, **19**, 17928–17936.
- 43 T. Lu and F. Chen, *J. Comput. Chem.*, 2012, **33**, 580–592.
- 44 W. Humphrey, A. Dalke and K. Schulten, *J. Mol. Graphics Modell.*, 1996, **14**, 33–38.
- 45 R. M. Sellers, *Analyst*, 1980, **105**, 950–954.
- 46 C. S. Pan and Y. F. Zhu, *Environ. Sci. Technol.*, 2010, **44**, 5570–5574.
- 47 Y. Shiraishi, S. Kanazawa, Y. Sugano, D. Tsukamoto, H. Sakamoto, S. Ichikawa and T. Hirai, *ACS Catal.*, 2014, **4**, 774–780.
- 48 L. Shi, L. Yang, W. Zhou, Y. Liu, L. Yin, X. Hai, H. Song and J. Ye, *Small*, 2018, **14**, 1703142.